Metal Binding Activity of the *Escherichia coli* Hydrogenase Maturation Factor HypB†

Michael R. Leach, Shaifali Sandal, Haowei Sun, and Deborah B. Zamble*

Department of Chemistry, University of Toronto, Toronto, Ontario, Canada M5S 3H6

Received May 26, 2005; Revised Manuscript Received July 3, 2005

ABSTRACT: The formation of the [NiFe] metallocenter of *Escherichia coli* hydrogenase 3 requires the participation of proteins encoded by the hydrogenase pleiotropy operon *hypABCDEF*. The insertion of Ni(II) into the precursor enzyme follows the incorporation of the iron center and is the function of HypA, a Zn(II)-binding protein, and HypB, a GTPase. The Ni(II) donor and the mechanism of transfer of Ni(II) into the hydrogenase precursor protein are not known. In this study, we demonstrate that HypB is a nickel-binding protein capable of binding 1 equiv of Ni(II) with a K_d in the sub-picomolar range. In addition, HypB has a weaker metal-binding site that is not specific for Ni(II) over Zn(II). Examination of the isolated C-terminal GTPase domain revealed that the high-affinity metal binding capability was severely abrogated but the low-affinity site was intact. By mutating conserved cysteine and histidine residues in *E. coli* HypB, we have localized the high-affinity Ni(II)-binding site to an N-terminal CXXCGC motif and the low-affinity metal-binding site to the GTPase domain. A model for the function of HypB during the Ni(II) loading of hydrogenase is proposed.

The biosynthesis of metalloenzymes often requires the cooperation of dedicated accessory proteins for the construction of the intricate catalytic centers (*1*, *2*). For example, sets of helper proteins have been identified that are essential for the production of nickel-containing enzymes such as urease, carbon monoxide dehydrogenase, acetyl-CoA synthase, and the [NiFe] hydrogenase (*2*−*4*). These proteins are responsible for gathering all of the components of the enzyme metallocenter and ensuring that they are correctly inserted into the enzyme precursor protein. In addition, GTP hydrolysis is necessary to complete the biosynthesis of these enzymes, and this reaction is catalyzed by the GTPase accessory proteins UreG, CooC, AcsF, and HypB (*4*−*9*). The mechanism by which nickel is inserted or how it is coupled to GTP hydrolysis is unknown in all four cases.

The heterodimeric *Escherichia coli* hydrogenase 3 is a part of the formate hydrogenlyase complex that links hydrogen gas production through proton reduction to formate oxidation (*10*). The hydrogenase 3 large subunit HycE contains the nickel and iron [NiFe] bimetallic active site (*11*, *12*). During biosynthesis, it is thought that the iron center is inserted first, followed by nickel insertion and then proteolytic cleavage of a C-terminal peptide by the peptidase HycI, which recognizes the nickel-bound state of hydrogenase 3 (for recent reviews, see refs *2*, *3*, *13*, and *14*). The *hyp* operon encodes the accessory proteins, HypABCDEF, which are all required for hydrogenase 3 biogenesis (*15*, *16*), and HypBDEF also act pleiotropically in the biosynthesis of other [NiFe] hydrogenase isoenzymes in *E. coli*. Both HypA and HypB are implicated in the nickel insertion step because the hydrogenase deficiencies of genetic mutants are at least partially complemented by supplementation of the growth media with excess nickel (*5*, *15*−*18*). HypA and its homologues have a weak affinity for nickel as well as a structural zinc site, and it has been suggested that this factor may act as an architectural component of the nickel insertion complex (*19*−*21*). Mutations of conserved residues in the GTPase motifs of HypB that result in the loss of GTPase activity in vitro also abrogate hydrogenase activity in vivo due to a lack of Ni(II) loading (*5*), indicating that GTP hydrolysis is required for the transfer of a nickel ion into the large subunit of hydrogenase.

Although binding of metal to *E. coli* HypB has not been previously observed (22), a distinctive feature of many HypB homologues from organisms other than *E. coli* is a polyhistidine stretch capable of binding nickel with high capacity but low affinity. For instance, the HypB protein of *Bradyrhizobium japonicum* has 24 His residues within a 39-amino acid stretch and is capable of binding 9 equiv of nickel with an average K_d of 2.3 μM (*23*). However, although removal of the histidine-rich region in HypB affects nickel storage in this organism, it does not completely abolish Ni(II) binding by the protein or affect the incorporation of Ni(II) into hydrogenase (*7*, *24*). Similar polyhistidine stretches are observed in accessory proteins for other nickel enzymes, such as UreE and CooJ from the urease and carbon monoxide dehydrogenase biosynthetic pathways, respectively (*3*). Again, the His-rich regions appear to be for nickel storage and can be separated from the nickel insertion activity (*3*). *E. coli* HypB does not have a similar domain, and nickel storage in this organism may be the role of the peptidyl-prolyl isomerase SlyD (*25*), which has a C-terminal domain, rich

† This work was supported in part by NSERC (Canada) and the Canada Research Chairs program. M.R.L. is supported by an NSERC postdoctoral fellowship, and S.S. and H.S. were supported by NSERC undergraduate summer fellowships.

* To whom correspondence should be addressed. Phone and fax: (416) 978-3568. E-mail: dzamble@chem.utoronto.ca.

10.1021/bi050993j CCC: $30.25
Published on Web 08/18/2005

Table 1: PCR Primers Used for Cloning and Mutagenesis[a]

name	sequence
HypB forward	5′-CAGGAGTG**ATTAAT**GTGTACAACATGCGGTTGC-3′
HypB reverse	5′-GATCTG**CTCGAG**AACGCCTATGCACATCGCTG-3′
G domain forward	5′-CCAGCG**ATTAAT**GCTGGAAGTCGAAATTG-3′
G domain reverse	5′-GTGGTG**CTCGAG**AACGCCTATG-3′
C2A forward	5′-GAAGGAGATATACATAATGgcTACAACATGCGGTTGCGG-3′
C2A reverse	5′-CCGCAACCGCATGTTGTAgcCCATTATGTATATCTCCTTC-3′
C5A forward	5′-CATAATGTGTACAACAgcCGGTTGCGGTGAAGGCAAC-3′
C5A reverse	5′-GTTGCCTTCACCGCAACCGgcTGTTGTACACATTATG-3′
C7A forward	5′-GTACAACATGCGGTgcCGGTGAAGGCAACCTGTATATC-3′
C7A reverse	5′-GATATACAGGTTGCCTTCACCGgcACCGCATGTTGTAC-3′
C166A forward	5′-GAACACCGGTAAAGGCgcCCATCTTGACGCACAG-3′
C166A reverse	5′-CTGTGCGTCAAGATGGgcGCCTTTACCGGTGTTC-3′
H167A forward	5′-CACCGGTAAAGGCTGCgcTCTTGACGCACAGATG-3′
H167A reverse	5′-CATCTGTGCGTCAAGAgcGCAGCCTTTACCGGTG-3′
C198A forward	5′-GTTGGCAACCTCGTAgcCCCGGCCAGCTTC-3′
C198A reverse	5′-GAAGCTGGCCGGGgcTACGAGGTTGCCAAC-3′
C2,7A forward	5′-GCTAACATGCGGTgcCGGTGAAGGCAACCTGTATATC-3′
C2,7A reverse	5′-GATATACAGGTTGCCTTCACCGgcACCGCATGTTGTAGC-3′
C2,5,7A forward	5′-CATAATGGCTACAACAgcCGGTGCCGGTGAAGGC-3′
C2,5,7A reverse	5′-GCCTTCACCGGCACCGgcTGTTGTAGCCATTATG-3′

[a] Restriction enzyme sites are shown in bold. Mutations are shown in lowercase. The double mutant C2,7A was generated by using C2A HypB-pET24b as template and the primers C2,7A forward and reverse. The triple mutant C2,5,7A was generated by using C2,7A HypB-pET24b as a template and the primers C2,5,7A forward and reverse.

in histidine, cysteine, and carboxylate residues, that is capable of binding three Ni(II) ions with micromolar affinity (*26*). A recent study demonstrated that SlyD binds to HypB and has a role in the nickel insertion step of hydrogenase biosynthesis (*27*), although its exact function remains to be defined.

HypB from *E. coli* was initially characterized as a homodimer with a weak K_d for GDP of 1.2 μM and a weak GTPase activity [$k_{cat} = 0.17$ min^{-1} and $K_m = 4$ μM (*22*)], and similar parameters have been reported for homologues from other organisms (*23*). To further understand the function of *E. coli* HypB in the hydrogenase maturation pathway, we examined its metal binding properties. This protein binds nickel with high affinity in a site at least partially composed of conserved cysteine residues at the immediate N-terminus. Furthermore, there is a second metal-binding site in the GTPase domain of HypB that binds metal with a substantially lower affinity and is not selective for nickel. These results support the hypothesis that HypB is involved in nickel loading of the hydrogenase and suggest that HypB may have a direct role in metal transfer. Possible functions of the two metal binding activities during hydrogenase biosynthesis are discussed.

EXPERIMENTAL PROCEDURES

Materials. Restriction endonucleases and T4 DNA ligase were obtained from New England Biolabs. *Pfu* DNA polymerase was purchased from Stratagene. All chromatography media were from Amersham Pharmacia Biotech. Kanamycin, TCEP,[1] and IPTG were purchased from BioShop (Toronto, ON). Metal salts were, as a minimum, 99.9% pure and purchased from Aldrich. Metal binding studies were performed with atomic absorption standard solutions, and other reagents were analytical grade from Sigma. Primers (Table 1) were purchased from Sigma Genosys. Buffers for all metal assays were treated with Chelex-100 (Bio-Rad) to minimize trace metal contamination. All the samples were prepared with Milli-Q water, 18.2 MΩ-cm resistance (Millipore).

HypB Expression Vector and Mutants. The coding sequence of HypB was amplified from *E. coli* (DH5α) chromosomal DNA by using primers (Table 1) designed with restriction sites for *Ase*I (HypB forward) and *Xho*I (HypB reverse). The digested PCR product was ligated with T4 DNA ligase into the pET24b vector (Novagen) digested with *Nde*I and *Xho*I. The HypB GTPase domain (G domain, residues 77−290) was PCR amplified from HypB-pET24b by using primers G domain forward and reverse, digested with *Ase*I and *Xho*I, and ligated into pET24b that had been digested with *Nde*I and *Xho*I. Point mutants were generated from the HypB-pET24b parent vector by using QuikChange PCR mutagenesis (Stratagene) with *Pfu* polymerase followed by *Dpn*I digestion. For routine handling, plasmids were transformed into XL-2 blue competent cells (Stratagene) and isolated by using the Qiagen plasmid mini-prep kit. All plasmids were sequenced in the forward and reverse directions (ACGT, Toronto, ON) by using T7 promoter and terminator primers to verify the cloned sequences and mutations.

Protein Expression and Purification. For expression of HypB or the G domain, the plasmids were transformed into BLR(DE3) cells (Novagen). Routinely, 1.5 L of LB medium, supplemented with 50 μg/mL kanamycin and 1 mM $NiSO_4$, was inoculated with 15 mL of an overnight culture and grown aerobically at 37 °C until the A_{600} reached 0.6, cooled to

[1] Abbreviations: DEAE, diethylaminoethyl; DTNB, 5,5′-dithiobis-(2-nitrobenzoic acid); DTT, dithiothreitol; EDDA, ethylenediamine-*N*,*N*′-diacetic acid; EDTA, ethylenediaminetetraacetic acid; EGTA, ethylene glycol bis(2-aminoethyl ether)-*N*,*N*,*N*′,*N*′-tetraacetic acid; ESI-MS, electrospray ionization mass spectrometry; FKBP, FK506-binding protein; G domain, GTPase domain of HypB consisting of residues 77−290; HEPES, 4-(2-hydroxyethyl)-1-piperazineethanesulfonic acid; HPLC, high-performance liquid chromatography; hyp, hydrogenase pleiotropy; ICP-AES, inductively coupled plasma-atomic emission spectroscopy; IPTG, isopropyl β-D-thiogalactoside; MG, Malachite Green; NTA, nitrilotriacetic acid; PAR, 4-(2-pyridylazo)resorcinol; PMB, *p*-hydroxymercuribenzoic acid; PMSF, phenylmethanesulfonyl fluoride; SDS−PAGE, sodium dodecyl sulfate−polyacrylamide gel electrophoresis; TCEP, tris(2-carboxyethyl)phosphine hydrochloride; Tris, tris(hydroxymethyl)aminomethane.

room temperature, and induced with 0.25 mM IPTG. After 4 h, the cells were harvested by centrifugation and resuspended in 20 mM Tris (pH 7.5) and 100 mM NaCl supplemented with 5 mM TCEP and 1 mM PMSF, sonicated on ice, and centrifuged at 18 000 rpm for 30 min at 4 °C. All subsequent steps were performed at 4 °C or on ice. The supernatant was passed through a 0.45 μm syringe filter before being loaded onto a DEAE Sepharose anion-exchange column equilibrated with buffer A [20 mM Tris (pH 7.5) and 1 mM TCEP]. Fractions from a NaCl gradient were screened by SDS−PAGE, and the HypB-containing fractions, at ∼250 mM NaCl, were pooled and dialyzed against buffer A. The dialyzed sample was loaded onto a HiTrapQ anion-exchange column equilibrated with buffer A, and HypB was eluted with a NaCl gradient. HypB fractions were pooled and concentrated for loading onto a Superdex 75 gel filtration column equilibrated with 25 mM HEPES (pH 7.6), 200 mM NaCl, and 1 mM TCEP. The gel filtration column was calibrated with bovine serum albumin, ovalbumin, trypsinogen, and lysozyme (Sigma). HypB and the G domain eluted at volumes consistent with molecular masses of ≈40 and ≈27 kDa, respectively, compared to their actual masses of 31.6 and 23.4 kDa, respectively, indicating that under these conditions the proteins exist as monomers. The protein concentration was determined by using the calculated extinction coefficient of 16 500 M^{-1} cm^{-1} at 280 nm (*28*). The free thiol content of HypB was quantified by reaction with DTNB in the presence of 6 M guanidinium hydrochloride and by using β-mercaptoethanol as a standard. Purified HypB preparations were generally >90% reduced prior to treatment with EDTA and TCEP (to prepare apo-HypB, see below) in the anaerobic glovebox and were 100% reduced after treatment. The molecular mass of purified HypB was determined by ESI-MS (Department of Chemistry, University of Toronto) to be 31 433 Da, lower than the predicted molecular mass of 31 565 Da by 132 Da, indicating the loss of the N-terminal methionine residue. The molecular masses of all point mutants, as determined by ESI-MS, were consistent with removal of their N-terminal methionine residues. By ESI-MS, the G domain had a mass of 23 442 Da compared to a predicted mass of 23 441 Da, indicating that it retained its N-terminal methionine residue. All proteins were >90% pure as estimated by Coomassie-stained SDS−PAGE.

Metal Analysis. For inductively coupled plasma-atomic emission spectroscopy (ICP-AES), samples were diluted to approximately 20 μM in buffer A and run on an Optima 3000DV instrument (Perkin-Elmer) equipped with a cross-flow nebulizer that was calibrated with standard metal stocks (Avery). An HPLC method developed in our laboratory was also employed as an alternative method of metal content determination that provides results comparable to those with ICP-AES (*29*). For HPLC analysis, 50 μg of protein was dried by centrifugation under vacuum, reconstituted with metal-free concentrated HCl (Seastar Chemicals), and hydrolyzed by incubation overnight at 95 °C. The sample was dried again to remove HCl and reconstituted in 80 μL of MilliQ water. This sample was injected onto an IonPak CS5A column attached to a metal-free Dionex BioLC HPLC system followed by postcolumn mixing with 4-(2-pyridylazo)-resorcinol (PAR) and detection at 500 nm.

Metal Titration and Competition Assay. Apo-HypB was generated by incubating HypB with 10 mM EDTA and 1 mM TCEP for 2−3 days in an anaerobic glovebox at 4 °C. EDTA and TCEP were removed by passing the protein sequentially over two PD-10 gel filtration columns (Amersham) equilibrated with 25 mM HEPES and 100 mM NaCl (pH 7.6) in the glovebox. Nickel was added to apo-HypB either in the presence or in the absence of competitor and incubated in the glovebox at 4 °C, and nickel binding was assessed by the absorbance signal at 320 nm compared to apo-HypB after removal of samples from the glovebox. For competitor studies, 1−10 mM EGTA was used and samples were incubated overnight at 4 °C. The metal affinity constants for the competitors described above were obtained from the National Institute of Science and Technology (NIST) database, version 7.0 (*30*), and protonation constants of the metal ions were obtained from Perrin and Dempsey (*31*). The apparent constants for the experimental conditions of pH 7.6 and an ionic strength of 0.1 were calculated using the equations described by Fahrni and O'Halloran (*32*). Using a $K_{d(app)}$ of EGTA for Ni(II), adjusted for a pH of 7.6, of 5.21×10^{-11} M (*33*) and an ϵ_{320} for Ni(II)-HypB of 7255 M^{-1} cm^{-1}, the concentrations of free nickel were determined by using the equation

$$([Me]_T - [MeHypB])[C]_T - [MeC][[C]_T + [Me]_T - [MeHypB] + K_{d(app)}] + [MeC]^2 = 0$$

where $[Me]_T$ is the total metal concentration, $[C]_T$ is the concentration of competitor, and [MeC] and [MeHypB] are the concentrations of metal−competitor and metal−protein complexes, respectively. This equation was solved for [MeC], and then the concentration of free metal [Me] was obtained by using the equation $[Me]_T = [Me] + [MeC] + [MeHypB]$. The data were fit to the equation $r = [Me]^n/(K_d^n + [Me]^n)$, where r is the fraction of protein bound to metal, [Me] is the free metal concentration, n is the Hill coefficient, and K_d is the free metal concentration required for 50% saturation.

To determine the affinity of the G domain for nickel, 10 μM apo-G domain was titrated with Ni(II) in the absence of competitor and the absorbance at 280 nm was monitored. The absorbance of the apo-protein was subtracted before fitting the data to the equation for r described above. To determine the affinity of zinc for the G domain, Zn(II) was titrated into a solution of 10 μM G domain in the presence of 10 equiv of nickel. The fractional saturation with nickel was determined by using A_{280} and fitting to a maximum possible saturation of 0.9 under these conditions, as determined from the calculated K_{Ni} of 12 μM. The data were fit to the equation

$$r = 1/[1 + (K_{Ni}/[Ni])(1 + [Zn]/K_{Zn})]$$

where r is the fractional saturation of the G domain with Ni(II) and K_{Ni} and K_{Zn} are the dissociation constants of G domain complexes with Ni(II) and Zn(II), respectively.

Release of Metal to PAR. Protein samples were diluted to 10 μM in buffer A followed by the addition of 100 μM PAR. The formation of the 2:1 PAR−metal complex in solution can be monitored at 500 nm (*34*). The concentration of the Ni(II)−PAR_2 complex was calculated by using an ϵ_{500} of 66 000 M^{-1} cm^{-1} determined from a standard Ni(II) curve

prepared under the same conditions. Metal release from HypB was monitored by the increase in the metal-bound PAR signal at 500 nm after blanking with PAR alone. The total amount of bound metal was determined by treating a parallel sample with excess *p*-hydroxymercuribenzoic acid (PMB) in the presence of PAR, and confirmed by a HPLC-PAR assay. Percent metal released ($\%M_{rel}$) was calculated from the absorbance values and then converted into percent metal bound ($\%M_{bound} = 100 - \%M_{rel}$) and normalized to the number of metal equivalents bound to the protein. Metal release curves were fit to a single- or double-exponential decay to determine metal dissociation rates (k_{off}). For metal release experiments in the presence of PMB, aliquots with 6.25 μM HypB were incubated with 0−16 equiv of PMB for 30 min at room temperature followed by the addition of 100 μM PAR. The absorbance at 500 nm was measured, and the data were converted to metal equivalents released by using the ϵ_{500} for the Ni(II)−PAR_2 complex mentioned above.

GTPase Activity. GTPase activity was determined by the Malachite Green (MG) assay for free phosphate adapted from Lanzetta et al. (*35*). To prepare the MG reagent, three parts 0.045% malachite green in water were mixed with one part 4.2% ammonium molybdate in 4 N HCl and allowed to stand for 20 min. The mixture was filtered through Whatman paper, and 0.2% Tween 20 was added. For time course reactions, 100 μL of the MG reagent was added to 25 μL aliquots of the reaction mixture, consisting of 200 μM GTP, approximately 5 μM protein, 50 mM Tris (pH 7.5), 50 mM KCl, and 5 mM $MgCl_2$, followed by 15 μL of 34% sodium citrate. Buffer-only and GTP-only controls were run to determine background signals. The amount of phosphate released was calculated on the basis of a standard curve from a phosphate standard (Molecular Probes).

Circular Dichroism Spectroscopy. Wild-type HypB and mutants were passed over a PD-10 gel filtration column pre-equilibrated with 20 mM potassium phosphate (pH 7.5), and 10−15 μM protein was analyzed on a Jasco J-170 spectropolarimeter with a 1 mm path length over a wavelength range of 200−250 nm at room temperature.

RESULTS

Stoichiometric Metal Binding to HypB. To determine if HypB binds nickel the protein was purified from cells grown and induced in medium supplemented with 1 mM $NiSO_4$, 1 mM $ZnSO_4$, or no additional metal. The protein was then subjected to metal analysis by two techniques, ICP-AES and/or HPLC-PAR (Table 2). If purified from cells grown aerobically in LB medium, conditions that do not induce expression of the Nik nickel transport system (*36*), HypB contained only trace amounts of Ni(II) and Zn(II), and significant amounts of iron (27 ± 6%). If purified from cells grown in LB medium supplemented with 1 mM Ni(II), HypB contained close to stoichiometric amounts of nickel (81 ± 3%) and 24 ± 10% Zn(II). The nickel-containing protein also exhibited an absorbance peak at 320 nm that could be eliminated by incubation with 10 mM EDTA for 3 days at 4 °C (data not shown and see below). HypB purified from cells grown in medium supplemented with 1 mM Zn(II) contained almost 1 equiv of Zn(II) (Table 2), indicating either that a second site exists or that the Ni(II)-binding site could also be loaded with Zn(II).

Table 2: Metal Analysis of HypB and HypB Mutants

protein[a]	metal added to media	% Ni(II)[c]	% Zn(II)
HypB (3)[d]	no metal added	3 ± 1	6 ± 3
HypB (3)	1 mM Zn(II)	n/d	71 ± 13
HypB (6)	1 mM Ni(II)	81 ± 3	24 ± 10
G domain (2)	1 mM Zn(II)	n/d[e]	42 ± 4
G domain (2)	1 mM Ni(II)	n/d[e]	1
C2A (3)[b]	1 mM Ni(II)	44 ± 2	16 ± 4
C5A (3)[b]	1 mM Ni(II)	40 ± 4	23 ± 6
C7A (3)[b]	1 mM Ni(II)	42 ± 6	26 ± 5
C2,7A (2)[b]	1 mM Ni(II)	7 ± 3	20 ± 7
C2,5,7A (2)[b]	1 mM Ni(II)	9 ± 2	14 ± 13
C166A (4)	1 mM Ni(II)	81 ± 7	11 ± 4
H167A (2)	1 mM Ni(II)	85 ± 5	10 ± 2
C198A (2)	1 mM Ni(II)	80 ± 6	3 ± 1

[a] Proteins purified from cells grown in LB media, with or without supplementation with 1 mM Ni(II) or Zn(II) as indicated, were analyzed for metal content. The number of replicates is given in parentheses. [b] These samples were analyzed by using the HPLC-PAR assay; all others were analyzed with ICP-AES. [c] The average percent metal ± standard deviation is reported. [d] HypB from cells grown in LB media with no added metal also contained 27 ± 6% iron. [e] Not detected.

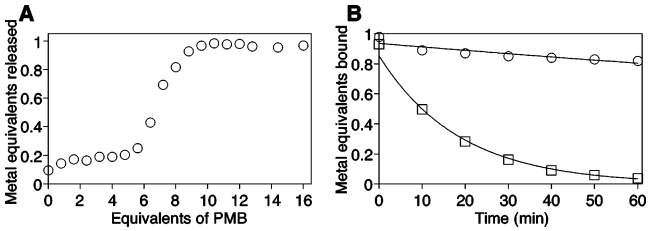

FIGURE 1: HypB uses thiolates to coordinate bound metal. (A) The incubation of 10 μM HypB purified from nickel-containing media (Table 2) with an increasing number of equivalents of PMB results in the release of metal to PAR as monitored by an increase in absorbance at 500 nm. By using an ϵ_{500} value for the Ni(II)−PAR_2 complex of 66 000 M^{-1} cm^{-1}, the absorbance values were converted into a Me(II)−PAR_2 concentration and expressed as a ratio of released metal to protein concentration. (B) The kinetics of the release of metal from HypB to PAR in the absence (○) or presence of 100 μM hydrogen peroxide (□) was monitored by using the absorbance of the Ni(II)−PAR_2 complex at 500 nm. The data were fit to an equation for single-exponential decay with $t_{1/2}$ values of 274 and 13 min for the release of metal in the absence and presence of hydrogen peroxide, respectively.

Thiolate-Containing Coordination Sphere. To investigate the nature of the metal-binding site of HypB, the nickel-containing purified protein was titrated with the thiol-reactive reagent PMB in the presence of the metallochromic indicator PAR. Only a small fraction of the metal bound to HypB was released into solution following the addition of up to 6 equiv of PMB, suggesting that six of the nine Cys residues of HypB may be more accessible and not involved in metal binding (Figure 1A). The balance of the bound metal was released upon the subsequent addition of an additional 3 equiv of PMB, demonstrating that at least one of the remaining three Cys residues is involved in metal coordination.

The involvement of Cys residues in metal coordination was also tested by incubating HypB with hydrogen peroxide. In the presence of PAR, only a small fraction of the metal was released from HypB over the course of 1 h (Figure 1B). In contrast, the incubation of 10 μM HypB with 100 μM hydrogen peroxide resulted in the rapid release of metal to PAR, decreasing the half-time of release ($t_{1/2}$) from 274 to 13 min at room temperature (Figure 1B). The formation of

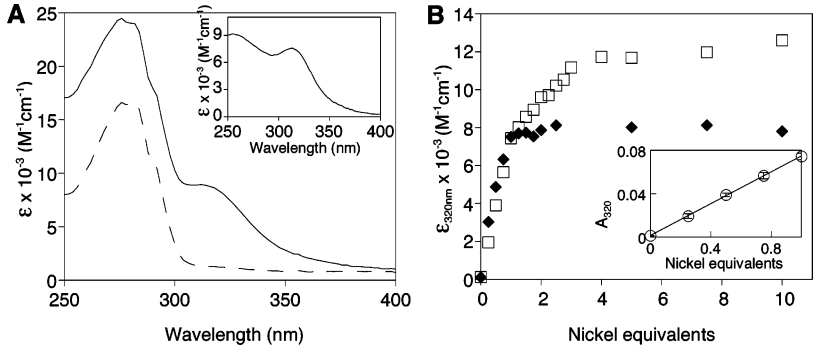

FIGURE 2: Binding of nickel to apo-HypB. (A) The incubation of HypB with 10 mM EDTA and 1 mM TCEP for 3 days at 4 °C eliminates the absorbance at 320 nm. Removal of EDTA by passing the apo-HypB sequentially over two PD-10 gel filtration columns in an anaerobic glovebox yields apo-HypB (− − −) that is competent to bind metal. The addition of 1 equiv of Ni(II) results in an increase in absorbance between 250 and 350 nm with a peak at 320 nm (—). A difference spectrum was generated by subtracting the signal of apo-HypB from that of HypB with 1 equiv of Ni(II) bound (inset). Metal analysis following gel filtration confirmed stoichiometric nickel binding (Table 3). (B) Titration of apo-HypB with up to 1 equiv of Ni(II) results in a linear titration curve (□ and inset), yielding an ϵ_{320} of $(7.3 \pm 0.1) \times 10^3$ M^{-1} cm^{-1} ($n = 6$). Further titration of apo-HypB with Ni(II) results in an increase in absorbance at 320 nm (□) that is not observed in the presence of 10 mM glycine (◆).

disulfide bonds in conjunction with metal release was confirmed by assaying for free thiol content with DTNB before and after the addition of hydrogen peroxide (data not shown). This oxidative metal release is comparable to the reactivity of Hsp33, a Zn(II)-binding redox-regulated chaperone of *E. coli* that releases its metal in response to cytosolic oxidative stress, a condition that is mimicked in vitro by the addition of hydrogen peroxide. In the case of Hsp33, a 40-fold excess of hydrogen peroxide results in disulfide bond formation concomitant with Zn(II) release at 43 °C with a $t_{1/2}$ of 16 min (*37*). These results indicate that HypB uses one or more thiolates in the coordination sphere of its bound nickel.

Nickel Titration of Apo-HypB. The metal bound to HypB could be removed by incubation with 10 mM EDTA followed by gel filtration to remove chelated metal and excess EDTA. Reloading of nickel onto apo-HypB prepared in this manner was not observed, however, probably due to the rapid oxidation of the apo-HypB cysteines. To avoid disulfide bond formation, HypB was incubated with 10 mM EDTA and 1 mM TCEP in an anaerobic glovebox for 2−3 days at 4 °C followed by gel filtration to remove metal, EDTA, and TCEP. The addition of 1 equiv of nickel under anaerobic conditions produced the characteristic electronic absorption band at 320 nm (Figure 2A). Upon titration of apo-HypB with increasing amounts of nickel, a linear increase in absorbance at 320 nm was observed up to 1 equiv, yielding an ϵ_{320} value of $(7.3 \pm 0.1) \times 10^3$ M^{-1} cm^{-1} (Figure 2B). Loading of apo-HypB with 1 equiv of Ni(II) followed by gel filtration revealed a metal content of 101 ± 3% by PAR analysis (Table 3) and an ϵ_{320} value of $(7.3 \pm 0.2) \times 10^3$ M^{-1} cm^{-1}, confirming that HypB tightly binds stoichiometric nickel.

Surprisingly, the titration of HypB with Ni(II) beyond 1 equiv resulted in a nonlinear increase in absorbance at 320 nm that saturated after the addition of more than 10 equiv (Figure 2B). In the presence of 10 mM glycine, a weak nickel competitor [log $K_a^{Ni} = 6.2$ (*38*)], the absorbance produced by 1 equiv of nickel was not affected, but no subsequent increase in the 320 nm signal was observed upon addition of more than stoichiometric amounts of nickel. These results suggest that HypB has two Ni(II)-binding sites, one of high affinity and one of low affinity. Metal analysis of apo-HypB incubated with a 20-fold excess of Ni(II) followed by gel filtration chromatography confirmed that HypB could bind 2 equiv of Ni(II) (Table 3). If gel filtration was followed by dialysis against metal-free buffer, however, only 1 equiv of Ni(II) remained bound, confirming that the second site is of lower affinity.

Table 3: Metal Content of Metal-Loaded HypB and HypB Mutants

protein	incubation conditions[a]	% metal content[b]
HypB	1 equiv of Ni(II)	101 ± 3
HypB	10 equiv of Ni(II)	164 ± 11
HypB	10 equiv of Ni(II)/dialysis[c]	95 ± 9
HypB	20 equiv of Ni(II)	190 ± 7
G domain	20 equiv of Ni(II)	107 ± 5
G domain	2 equiv of Zn(II)	92 ± 6
C2A	20 equiv of Ni(II)	196 ± 7
C5A	20 equiv of Ni(II)	201 ± 5
C7A	20 equiv of Ni(II)	191 ± 8
C2,7A	20 equiv of Ni(II)	142 ± 11
C2,5,7A	20 equiv of Ni(II)	106 ± 4
C166A	20 equiv of Ni(II)	99 ± 5
H167A	20 equiv of Ni(II)	93 ± 8
C198A	20 equiv of Ni(II)	183 ± 9

[a] Apo-HypB and HypB mutants were incubated with the indicated number of metal equivalents overnight at 4 °C in an anaerobic glovebox. The metal-loaded proteins were then passed over a PD-10 gel filtration column to remove unbound metal. [b] The metal content of the proteins was determined by incubation of an aliquot with 50 μM PAR in the presence 6 M guanidinium chloride overnight and by using an ϵ_{500} of 66 000 M^{-1} cm^{-1} for the Ni(II)−PAR_2 and Zn(II)−PAR_2 complexes. Data are listed with average error for duplicate samples. [c] This sample had an additional dialysis step against a 2000-fold excess of metal-free buffer.

Affinity of HypB for Stoichiometric Nickel. To measure the affinity of HypB for stoichiometric nickel, nickel reconstitution of apo-HypB was repeated in the presence of metal-chelating competitors. The absorbance at 320 nm was used to measure the fraction of metal bound to HypB, and in these experiments, there was no spectroscopic evidence for a second metal binding to the protein. The affinity of the chelator EDTA for nickel was too strong to be of use (data not shown), while that of glycine was too weak (Figure 2B). HypB could compete with 5 mM EGTA, and detailed analysis revealed that HypB binds nickel with a K_d of $(1.3 \pm 0.2) \times 10^{-13}$ M (Figure 3). To ensure that the presence of a Ni(II)−HypB−EGTA ternary complex did not affect the

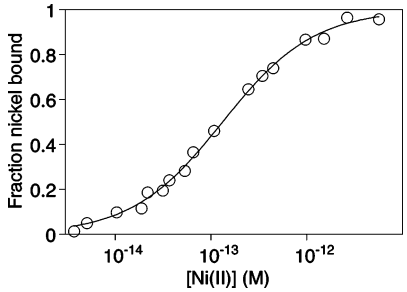

FIGURE 3: Metal affinity of HypB for Ni(II). Titration of 10 μM apo-HypB with Ni(II) was performed in the presence of 5 mM EGTA as a competitor and monitored at 320 nm. Data from several experiments such as that shown were fit to a Hill equation as described in Experimental Procedures to calculate a K_d of (1.3 $\pm$ 0.2) $\times$ 10^{-13} M and a Hill constant of 1.01 $\pm$ 0.06.

results, the experiment was repeated in the presence of 1 and 10 mM EGTA, yielding K_d values of (1.2 $\pm$ 0.2) $\times$ 10^{-13} and (1.2 $\pm$ 0.3) $\times$ 10^{-13} M, respectively (data not shown).

Metal Binding to the GTPase Domain. The GTPase activity of HypB is contained within the C-terminus of the protein, and the intact domain can be separated from the rest of HypB following tryptic digestion at residue 76 (ref *5* and our data not shown). To determine whether this fragment was capable of binding metal, the GTPase domain (G domain) starting at residue 77 was cloned and expressed with either 1 mM $NiSO_4$ or $ZnSO_4$ added to the growth media. Nickel was not detected in protein expressed in the presence of nickel, which only contained trace amounts of Zn(II) (Table 2). If the media were supplemented with 1 mM Zn(II), however, the purified G domain had a Zn(II) content of 42 $\pm$ 4%, suggesting that the G domain of HypB might contain a weak site for Zn(II).

The quantitative metal binding that is observed upon titration of full-length HypB with nickel was not detected upon the addition of stoichiometric nickel to the apo-G domain, suggesting that the high-affinity site was missing or significantly disrupted by the truncation. However, the addition of excess nickel to apo-G domain (Figure 4A) resulted in an increase in absorbance with a λ_{max} of 305 nm. The metal content of the G domain incubated with excess Ni(II) followed by gel filtration to remove unbound metal was 107 $\pm$ 5% (Table 3), confirming that the G domain possesses one Ni(II)-binding site per monomer. In addition, the difference spectrum derived from subtracting the spectrum of full-length HypB in the presence of a 25-fold excess of Ni(II) from that of HypB loaded with 1 equiv of Ni(II) is similar to that of the G domain in the presence of a 25-fold excess of Ni(II) subtracted from apo-G domain (Figure 4A inset and data not shown), suggesting that the second metal site is intact in the isolated G domain. Titration of the protein with Ni(II) revealed a $K_{d(app)}$ of (1.2 $\pm$ 0.2) $\times$ 10^{-5} M and a Hill coefficient of 1.2 $\pm$ 0.1 (Figure 4B).

Metal Selectivity of HypB and the G Domain. To investigate the selectivity of metal binding to HypB, 10 μM apo-HypB was incubated with Ni(II) in the presence of Zn(II), which does not have a detectable spectroscopic signal when bound to HypB. Titration of apo-HypB with nickel in the presence of 2 equiv of zinc does not affect the quantitative binding of 1 equiv of nickel (data not shown and Figure 5A), and the same titration curve as that produced from nickel titration in the presence of 10 mM glycine is observed (data not shown), indicating nickel selectivity at the high-affinity site but competition for the second nickel-binding site. To confirm that the second metal site in the G domain can bind zinc, the protein was incubated with just 2 equiv of Zn(II) followed by gel filtration, and the metal content was 92 $\pm$ 6% (Table 3). The addition of larger amounts of Zn(II) was precluded by protein precipitation. Furthermore, the addition of Zn(II) to the apo-G domain in the presence of 10 equiv of Ni(II) resulted in a concentration-dependent drop in absorbance at 280 nm (Figure 5B). An apparent K_d for Zn(II) of 1 μM was determined by fitting these data to a two-metal binding equation, an affinity 10-fold higher than that observed for nickel. These results demonstrate that the second metal-binding site is not selective for Ni(II) over Zn(II).

N-Terminal Cysteine Mutants. The nickel titrations of the C-terminal G domain in comparison with full-length HypB suggest that critical residues for the high-affinity nickel-binding activity are in the N-terminal domain of the protein. Furthermore, the experiments described above indicate that the coordination sphere of this site contains cysteine residues. Given these pieces of information, a likely metal-binding sequence is the N-terminal CXXCGC motif (with a loss of the initial methionine), which is conserved in most HypB homologues from eubacteria (*39*). To test this hypothesis, single- and multiple-alanine mutants of these cysteine residues were expressed and purified in the same manner as wild-type HypB. To ensure that these mutations did not

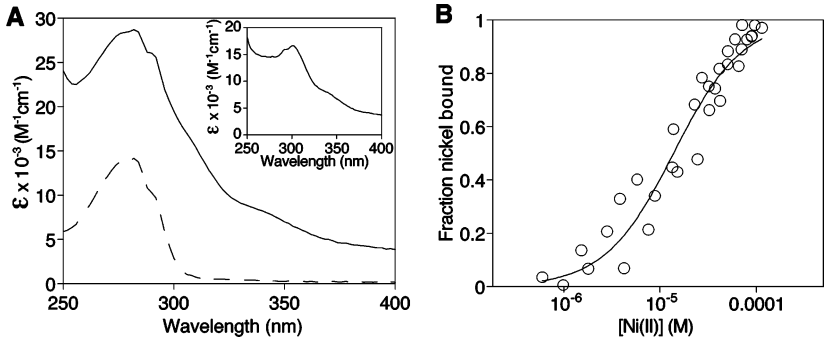

FIGURE 4: Nickel binding to the G domain. (A) The addition of 20 equiv of Ni(II) to the apo-G domain (– – –) resulted in an increase in absorbance between 250 and 400 nm with a maximum at 305 nm (—); the difference spectrum is shown in the inset. Metal analysis following gel filtration confirmed stoichiometric nickel binding (Table 3). (B) Direct Ni(II) titration of 10 μM apo-G domain was monitored by the increase in absorbance at 280 nm. After the free Ni(II) concentration had been adjusted for the Ni(II) bound to the G domain, the data from several experiments such as the one shown were fit to a Hill equation yielding a $K_{d(app)}$ of (1.2 $\pm$ 0.2) $\times$ 10^{-5} M and a Hill coefficient of 1.2 $\pm$ 0.1.

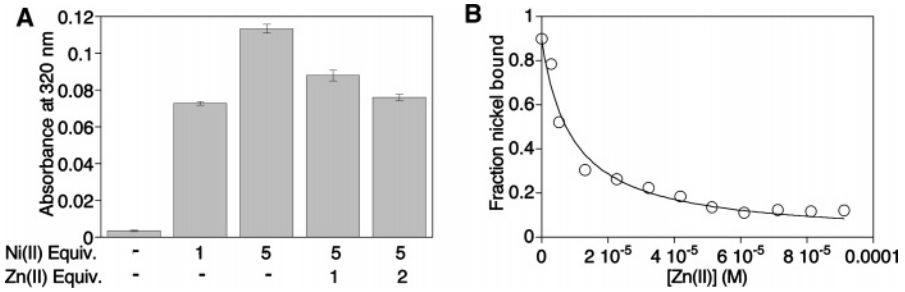

FIGURE 5: Effect of Zn(II) on Ni(II) binding to HypB and G domain. (A) Full-length apo-HypB (10 μM) was incubated overnight at 4 °C in an anaerobic glovebox with the indicated amounts of Ni(II) or Zn(II) followed by measurement of the absorbance at 320 nm. The values are averages from two experiments, and error bars represent the standard deviation. (B) The apo-G domain (10 μM) was incubated as described above with 10 equiv of Ni(II) in the presence of increasing amounts of Zn(II) prior to measuring the absorbance at 280 nm. The absorbance of the apo-G domain at 280 nm was subtracted and the net absorbance used to determine the fractional saturation with Ni(II). After the free Zn(II) concentration had been adjusted for the Zn(II) bound to the G domain, the data from several experiments such as the one shown were fit as described in Experimental Procedures to calculate a K_d of $(1.1 \pm 0.1) \times 10^{-6}$ M for Zn(II) binding to the G domain.

grossly alter the structure of HypB, the GTPase activity was quantified by using the Malachite Green colorimetric assay for free phosphate to determine if the turnover number differed from the value of 0.17 ± 0.3 min^{-1} measured for wild-type HypB (ref *22* and data not shown). The measured GTPase activities of apo-HypB, the G domain, or the site-specific mutants did not differ significantly from that of HypB purified with bound metal (data not shown). In addition, the CD spectrum of C2,5,7A-HypB was unchanged from that of HypB, confirming that these mutations do not affect the secondary structure of HypB (data not shown).

As purified, the single N-terminal mutants, C2A-, C5A-, or C7A-HypB, had significantly smaller amounts of bound Ni(II) than wild-type HypB (Table 2). To examine the metal-binding activity of these N-terminal cysteine mutants, the apoprotein was prepared in the same manner as described for wild-type HypB. Incubation with 20 equiv of Ni(II) followed by gel filtration revealed approximately 2 equiv of nickel bound to the single-cysteine mutants, indicating that they still retained two metal-binding sites (Table 3). However, upon addition of stoichiometric nickel, none of the mutants exhibited the intense electronic absorption signal at 320 nm observed for the wild-type protein (data not shown), indicating that the high-affinity site has been severely compromised. Titration of these mutants beyond 1 equiv of Ni(II) resulted in an absorbance signal that was similar to that observed upon titration of the G domain, and none of these mutants were able to compete with 1 mM EGTA for Ni(II) (data not shown). Upon incubation of C2,7A with excess nickel, only an average of one and one-half metal ions was detected, and analysis of the triple mutant C2,5,-7A revealed only stoichiometric metal bound (Table 3), indicating complete disruption of one of the metal-binding sites.

Metal Release Kinetics. To further investigate the relative metal affinities of HypB and the N-terminal cysteine mutants, the time course of metal release from protein to PAR was monitored at 500 nm and the data were fit to double-exponential decay curves (Figure 6). The wild-type and single-cysteine mutants were first loaded with 2 equiv of nickel, and the double mutant only had ~1.5 equiv of nickel bound (Table 3). In all cases, 1 equiv of Ni(II) was released from the low-affinity binding site with a $t_{1/2}$ of <1 min. Ni-(II) then slowly dissociated from the high-affinity binding site of wild-type HypB with a $t_{1/2}$ of 100 min, while the

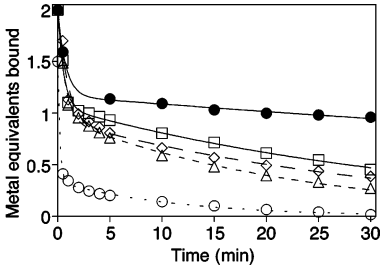

FIGURE 6: Kinetics of Ni(II) release of N-terminal cysteine point mutants compared to that of wild-type HypB. Aliquots of apo-HypB (●) or N-terminal cysteine mutants C2A, C5A, C7A, and C2,7A (□, ◇, △, and ○, respectively) were incubated overnight at 4 °C with a 20-fold excess of Ni(II) and then passed over a PD-10 gel filtration column, all in an anaerobic glovebox. These Ni(II)-loaded proteins were incubated with 100 μM PAR, and the time course of metal release was monitored at 500 nm. The amount of metal released was calculated by using an ϵ_{500} of 66 000 M^{-1} cm^{-1} for the Ni(II)−PAR$_2$ complex and then subtracted from the metal content of each protein (Table 3) to determine the amount of metal bound to the protein. The data were fit to double-exponential curves, revealing that 1 equiv of Ni(II) was released from all proteins with a $t_{1/2}$ of <1 min. The second half-life measured was 100, 26, 23, 16, and 8 min for wild-type HypB and C2A-, C5A-, C7A-, and C2,7A-HypB, respectively.

second Ni(II) bound to C2A-, C5A-, and C7A-HypB dissociated more rapidly with $t_{1/2}$ values of 26, 23, and 16 min, respectively. These experiments suggest that each one of these cysteines contributes to the high-affinity metal-binding site. The double mutant C2,7A-HypB exhibits even faster metal release kinetics with a $t_{1/2}$ of 8 min, indicating that mutation of two putative ligands results in an additive loss of affinity. As expected, nickel-loaded triple mutant C2,5,7A-HypB had ~1 equiv of bound metal after gel filtration (Table 3) and exhibited extremely fast metal release kinetics with a $t_{1/2}$ of 1 min (data not shown).

G Domain Mutants of HypB. Nickel titration of the G domain suggested that the second, lower-affinity metal-binding site was completely contained in this fragment of HypB. To test this hypothesis, mutations were prepared in the full-length protein at several absolutely conserved residues, C166, H167, and C198. All three purified mutants contained almost stoichiometric levels of nickel when expressed in media containing 1 mM $NiSO_4$ (Table 2), just like wild-type HypB, and none of these mutations affected either the GTPase activity or the overall secondary structure (data not shown). Titration of the apo-proteins with up to 1

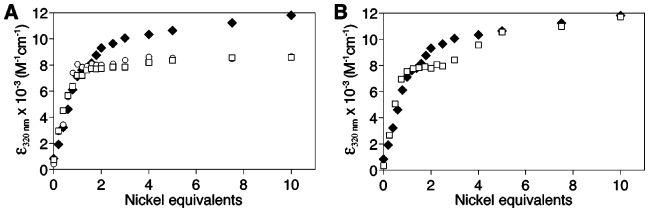

FIGURE 7: Effect of mutating conserved G domain cysteines on Ni(II) binding. (A) Ni(II) was titrated into 10 μM aliquots of apo-HypB (◆), C166A-HypB (○), and H167A-HypB (□) and incubated overnight at 4 °C in an anaerobic glovebox. The absorbance at 320 nm was measured for each aliquot and plotted against the number of equivalents of Ni(II) added. (B) Aliquots of apo-HypB (◆) and C198A-HypB (□) were incubated as described above.

equiv of Ni(II) revealed similar quantitative nickel binding to that observed upon titration of wild-type HypB, with an ϵ_{320} of approximately 7.2×10^3 M^{-1} cm^{-1} (Figure 7A,B). That the high-affinity site for C166A-, H167A-, or C198A-HypB is not disrupted is confirmed by Ni(II) competition experiments with 10 mM EGTA that yielded K_d values of $(1.2 \pm 0.1) \times 10^{-13}$, $(1.0 \pm 0.3) \times 10^{-13}$, and $(1.2 \pm 0.2) \times 10^{-13}$ M, respectively. Strikingly, titration of C166A-HypB and H167A-HypB beyond 1 equiv of Ni(II) does not result in a significant increase in absorbance at 320 nm (Figure 7A), indicating that mutation of these conserved residues disrupts the weak metal-binding site of HypB. In contrast, nickel titration of C198A-HypB clearly demonstrates two separate binding events (Figure 7B). Although upon saturation the intensity of the electronic absorption spectrum is unchanged, the interval between filling the first and second sites of C198A-HypB is more discrete compared to that observed in wild-type HypB, suggesting that the affinity of the second site has been weakened.

DISCUSSION

HypB is an essential protein for [NiFe] hydrogenase biosynthesis, and it is well established that the GTPase activity of the protein is critical for the nickel insertion step of this pathway (*5*, *7*, *9*, *19*). There is also evidence to suggest that some HypB homologues are responsible for nickel donation to the hydrogenase precursor (*7*, *24*). However, in the case of the *E. coli* protein, metal binding had not been previously observed, so it was not clear if it served a similar purpose. The experiments in this study demonstrate not only that *E. coli* HypB binds nickel but also that the protein has two metal-binding sites, a high-affinity nickel-binding site at the N-terminus of the protein and a low-affinity site in the G domain. These studies suggest that the nickel insertion function of this accessory protein is conserved in *E. coli*, and support the model in which the role of HypB during the transfer of nickel to hydrogenase involves a metal-binding site beyond the polyhistidine stretches found in many of the other HypB homologues (*7*).

Metal binding to HypB is very sensitive to the rapid oxidation that occurs under atmospheric conditions, which may explain why nickel binding was not previously observed (*22*). However, the hydrogenase enzymes in *E. coli* are expressed as components of anaerobic metabolism (*10*), so this sensitivity of HypB to oxygen would not hinder hydrogenase biosynthesis. Whether disulfide bond formation and the concomitant metal release is a regulatory response as suggested for proteins such as Hsp33 (*40*) will have to be investigated further. HypB binds the first nickel ion with sub-picomolar affinity, and mutagenesis studies suggest that the three conserved cysteine residues in the N-terminus of HypB, C2A, C5A, and C7A are the putative thiolate ligands. Given the fact that this N-terminal CXXCGC motif is not completely conserved in all bacterial HypB proteins and is lacking in archaeal HypB proteins (*39*), it is likely that this activity is dispensable to some degree and only required under certain growth conditions.

Possible functions of this high-affinity nickel-binding site of *E. coli* HypB include structural and/or regulatory roles. It is also feasible that this site is the source of nickel for the hydrogenase enzyme, particularly if the nickel concentrations in the prokaryotic cytosol are limited. Under such conditions, the N-terminus of HypB would be preferentially loaded over weaker sites that have K_d values in the micromolar range. In this model, the accessory protein HypA or a homologue could direct Ni(II)-bound HypB to the iron-loaded site of the hydrogenase large subunit (*19*−*21*), and the weak nickel-binding activity of HypA may cooperate with HypB during nickel insertion (*19*−*21*). The extremely tight nickel binding of isolated HypB suggests that if the high-affinity site supplies the nickel ion for the hydrogenase then some event is required to trigger metal release from HypB and insertion into the hydrogenase precursor protein. Although the nature of this trigger is not yet clear, it could involve a protein conformational change upon interaction with the hydrogenase metallocenter assembly complex, resulting in ligand exchange with the hydrogenase cysteine ligands, followed by an irreversible step such as GTP hydrolysis and/or cleavage of the C-terminal peptide of hydrogenase by HycI. It is also tempting to speculate that the peptidyl-prolyl isomerase activity of SlyD, which forms a complex with HypB (*27*), could be involved in catalyzing metal release from HypB. The potential roles of HypA and SlyD in modulating the high-affinity Ni(II) site of HypB and as metallochaperones of the nickel transfer process remain to be further examined. Finally, it should be noted that HypB may function as a dimer. Although dimerization was not detected under the gel filtration conditions used in this study, previous reports have demonstrated that HypB can form homodimers (*19*, *22*, *23*), indicating that further analysis is required to delineate the factors that affect the quaternary structure of the protein.

Tight metal binding to a terminal domain or a surface-exposed loop that is responsible for metal delivery is not unprecedented in metallochaperones (*2*). For example, the copper metallochaperone for copper−zinc superoxide dismutase (CCS) has two metal-binding sites, one each in N-terminal domain I and C-terminal domain III (*1*, *41*). In the case of CCS, it has been suggested that Cu(I) is transferred from domain I to domain III, which then pivots around to insert the metal into the enzyme active site. Other high-affinity metal-binding sites have been described at the immediate N-terminus of metalloproteins. The ATCUN [amino-terminal copper (Cu), nickel-binding] motif, NH_2-XXH, where X is any amino acid (*42*), found on serum albumin is capable of tightly binding to transition metals (*43*) in a coordination sphere made up of the amino-terminal nitrogen, two amide nitrogens, and the imidazole. For HypB, whether the terminal amino group or an amide nitrogen serves as a nickel ligand, or if other residues are involved in nickel binding, remains to be established.

An N-terminal truncation of HypB was used to localize the second metal-binding site to the C-terminal G domain, and mutagenesis suggests that the conserved C166 and H167 are ligands. A feasible role for the low-affinity metal-binding site is that it detects the properly loaded nickel site and activates an increase in its inherently sluggish GTP hydrolysis rate. GTP hydrolysis by HypB could then induce a conformational change that drives the release of the nickel insertion accessory proteins from the surface of the large subunit, allowing for proteolytic cleavage by HycI and complex formation with the small subunit of the enzyme. The relative contribution of the two metal sites of HypB during hydrogenase activation in vivo will be examined in a subsequent study.

HypB belongs to the G3E subclass of SIMIBI (signal recognition particle, MinD and BioD) GTPases that also includes the GTPase involved in the biosynthesis of the nickel enzyme urease (UreG) (*44*). Examination of UreG sequences reveals that they contain an absolutely conserved Cys-Pro-His (CPH) motif that is approximately 30 amino acids to the N-terminal side of the GTPase G3 motif, a position equivalent to that of C166 and H167 in HypB. A recent study of UreG from *Bacillus pasteurii* demonstrated that this GTPase binds Zn(II) with micromolar affinity (*45*). On the basis of the results presented here, it would be intriguing to determine if the CPH motif of UreG was involved in metal binding. The exact role of the metal-binding residues in this family of GTPases is still a subject of speculation, but it is interesting to note that mutation of conserved cysteines in a similar location of the GTPase involved in production of an iron-containing nitrile hydratase blocks expression of the active enzyme (*46*).

During production of the urease enzyme, the metal-binding accessory protein UreE is proposed to act as the source of nickel (*3*, *47*). UreE of *Klebsiella aerogenes* is able to stimulate nickel transfer to a complex of UreDFG and apourease even in the presence of chelators, supporting its putative role as a nickel donor (*48*). Intriguingly, *Helicobacter pylori* expressing GTPase-deficient mutants of HypB are severely deficient in urease activity (*49*), demonstrating that HypB also plays a role in urease production, at least in this organism. Although there is a formal possibility that HypB and not UreE acts as a nickel donor for the urease system in this organism, it is not likely because *H. pylori* HypB is one of the few homologues that does not contain either the N-terminal CXXCGC motif shown here to be involved in high-affinity nickel binding or a polyhistidine stretch. One would assume, then, that *H. pylori* HypB would, like *B. pasteurii* UreG, possess only a weak metal-binding site with a higher affinity for Zn(II) than for Ni(II), although metal binding to this protein has not been detected (*19*). It is clear that the detailed roles of HypB in the maturation of nickel enzymes, and how they differ in the context of various organisms, remain to be explored.

ACKNOWLEDGMENT

We thank Obina Onuora and Alexander Williams for the initial cloning and purification of *E. coli* HypB, Anelia Atanassova for performing HPLC-PAR analysis, and members of the Zamble lab for helpful discussions.

REFERENCES

1. Rosenzweig, A. C. (2002) Metallochaperones: Bind and deliver, *Chem. Biol. 9*, 673−677.
2. Kuchar, J., and Hausinger, R. P. (2004) Biosynthesis of metal sites, *Chem. Rev. 104*, 509−526.
3. Mulrooney, S. B., and Hausinger, R. P. (2003) Nickel uptake and utilization by microorganisms, *FEMS Microbiol. Rev. 27*, 239−261.
4. Loke, H. J., and Lindahl, P. A. (2003) Identification and preliminary characterization of AcsF, a putative Ni-insertase used in the biosynthesis of acetyl-CoA synthase from *Clostridium thermoaceticum*, *J. Inorg. Biochem. 93*, 33−40.
5. Maier, T., Lottspeich, F., and Böck, A. (1995) GTP hydrolysis by HypB is essential for nickel insertion into hydrogenases of *Escherichia coli*, *Eur. J. Biochem. 230*, 133−138.
6. Moncrief, M. B. C., and Hausinger, R. P. (1997) Characterization of UreG, identification of UreD-UreF-UreG complex, and evidence suggesting that a nucleotide-binding site in UreG is required for in vivo metallocenter assembly of *Klebsiella aerogenes* urease, *J. Bacteriol. 179*, 4081−4086.
7. Olson, J. W., and Maier, R. J. (2000) Dual roles of *Bradyrhizobium japonicum* nickelin protein in nickel storage and GTP-dependent Ni mobilization, *J. Bacteriol. 182*, 1702−1705.
8. Jeon, W. B., Cheng, J., and Ludden, P. W. (2001) Purification and characterization of membrane-associated CooC protein and its functional role in the insertion of nickel into carbon monoxide dehydrogenase from *Rhodospirillum rubrum*, *J. Biol. Chem. 276*, 38602−38609.
9. Mehta, N., Benoit, S., and Maier, R. J. (2003) Roles of conserved nucleotide-binding domains in accessory proteins, HypB and UreG, in the maturation of nickel-enzymes required for efficient *Helicobacter pylori* colonization, *Microb. Pathog. 35*, 229−334.
10. Böck, A., and Sawers, G. (1996) in *Escherichia coli and Salmonella, Cellular and Molecular Biology* (Neidhardt, F. C., Ed.) ASM Press, Washington, DC.
11. Vignais, P. M., Billoud, B., and Meyer, J. (2001) Classification and phylogeny of hydrogenases, *FEMS Microbiol. Rev. 25*, 455−501.
12. Volbeda, A., and Fontecilla-Camps, J. C. (2003) The active site and catalytic mechanism of NiFe hydrogenases, *Dalton Trans.*, 4030−4038.
13. Casalot, L., and Rousset, M. (2001) Maturation of the [NiFe] hydrogenases, *Trends Microbiol. 9*, 228−237.
14. Blokesch, M., Paschos, A., Theodoratou, E., Bauer, A., Hube, M., Huth, S., and Böck, A. (2002) Metal insertion into NiFe-hydrogenases, *Biochem. Soc. Trans. 30*, 674−680.
15. Lutz, S., Jacobi, A., Schlensog, V., Böhm, R., Sawers, G., and Böck, A. (1991) Molecular characterization of an operon (hyp) necessary for the activity of the three hydrogenase isoenzymes in *Escherichia coli*, *Mol. Microbiol. 5*, 123−135.
16. Jacobi, A., Rossmann, R., and Böck, A. (1992) The *hyp* operon gene products are required for the maturation of catalytically active hydrogenase isoenzymes in *Escherichia coli*, *Arch. Microbiol. 158*, 444−451.
17. Waugh, R., and Boxer, D. H. (1986) Pleiotropic hydrogenase mutants of *Escherichia coli* K12: Growth in the presence of nickel can restore hydrogenase activity, *Biochimie 68*, 157−166.
18. Hube, M., Blokesch, M., and Böck, A. (2002) Network of hydrogenase maturation in *Escherichia coli*: Role of accessory proteins HypA and HypF, *J. Bacteriol. 184*, 3879−3885.
19. Mehta, N., Olson, J. W., and Maier, R. J. (2003) Characterization of the *Helicobacter pylori* nickel metabolism accessory proteins needed for maturation of both urease and hydrogenase, *J. Bacteriol. 185*, 726−734.
20. Blokesch, M., Rohrmoser, M., Rode, S., and Böck, A. (2004) HybF, a zinc-containing protein involved in NiFe hydrogenase maturation, *J. Bacteriol. 186*, 2603−2611.
21. Atanassova, A., and Zamble, D. B. (2005) *Escherichia coli* HypA is a zinc metalloprotein with weak affinity for nickel, *J. Bacteriol. 187*, 4689−4697.
22. Maier, T., Jacobi, A., Sauter, M., and Böck, A. (1993) The product of the *hypB* gene, which is required for nickel incorporation into hydrogenases, is a novel guanine nucleotide-binding protein, *J. Bacteriol. 175*, 630−635.
23. Fu, C., Olson, J. W., and Maier, R. J. (1995) HypB protein of *Bradyrhizobium japonicum* is a metal-binding GTPase capable

of binding 18 divalent nickel ions per dimer, *Proc. Natl. Acad. Sci. U.S.A. 92*, 2333−2337.
24. Olson, J. W., Fu, C., and Maier, R. J. (1997) The HypB protein from *Bradyrhizobium japonicum* can store nickel and is required for the nickel-dependent transcriptional regulation of hydrogenase, *Mol. Microbiol. 24*, 119−128.
25. Roof, W. D., Horne, S. M., Young, K. D., and Young, R. (1994) *slyD*, a host gene required for ϕX174 lysis, is related to the FK506-binding protein family of peptidyl-prolyl cis-trans-isomerases, *J. Biol. Chem. 269*, 2902−2910.
26. Hottenrott, S., Schumann, T., Plückthun, A., Fischer, G., and Rahfeld, J.-U. (1997) The *Escherichia coli* SlyD is a metal ion-regulated peptidyl-prolyl *cis/trans*-isomerase, *J. Biol. Chem. 272*, 15697−15701.
27. Zhang, J. W., Butland, G., Greenblatt, J. F., Emili, A., and Zamble, D. B. (2005) A role for SlyD in the *Escherichia coli* hydrogenase biosynthetic pathway, *J. Biol. Chem. 280*, 4360−4366.
28. Gill, S. C., and von Hippel, P. H. (1989) Calculation of protein extinction coefficients from amino acid sequence data, *Anal. Biochem. 182*, 319−326.
29. Atanassova, A., Lam, R., and Zamble, D. B. (2004) A high-performance liquid chromatography method for determining transition metal content of proteins, *Anal. Biochem. 335*, 103−111.
30. Martell, A. E., and Smith, R. M. (2003) *NIST Standard Reference Database 46*, version 7.0, National Institute of Standards and Technology, Rockville, MD.
31. Perrin, D. D., and Dempsey, B. (1974) *Buffers for pH and metal ion control*, Chapman and Hall, London.
32. Fahrni, C. J., and O'Halloran, T. V. (1999) Aqueous coordination chemistry of quinoline-based fluorescence probes for the biological chemistry of zinc, *J. Am. Chem. Soc. 121*, 11448−11458.
33. Wang, S. C., Dias, A. V., Bloom, S. L., and Zamble, D. B. (2004) The selectivity of metal binding and the metal-induced stability of *Escherichia coli* NikR, *Biochemistry 43*, 10018−10028.
34. Hunt, J. B., Neece, S. H., and Ginsburg, A. (1985) The use of 4-(2-pyridylazo)resorcinol in studies of zinc release from *Escherichia coli* aspartate transcarbamoylase, *Anal. Biochem. 146*, 150−157.
35. Lanzetta, P. A., Alvarez, L. J., Reinach, P. S., and Candia, O. A. (1979) An improved assay for nanomole amounts of inorganic phosphate, *Anal. Biochem. 100*, 95−97.
36. Wu, L. F., and Mandrand-Berthelot, M.-A. (1986) Genetic and physiological characterization of new *Escherichia coli* mutants impaired in hydrogenase activity, *Biochimie 68*, 167−179.
37. Graf, P. C. F., Martinez-Yamout, M., VanHaerents, S., Lilie, H., Dyson, H. J., and Jakob, U. (2004) Activation of the redox-regulated chaperone Hsp33 by domain unfolding, *J. Biol. Chem. 279*, 20529−20538.
38. Martin, R. B. (1964) *Introduction to Biophysical Chemistry*, McGraw-Hill, New York.
39. Robson, R. (2001) in *Hydrogen as a fuel: Learning from nature* (Cammack, R., Frey, M., and Robson, R., Eds.) pp 57−72, Taylor & Francis, New York.
40. Graf, P. C. F., and Jakob, U. (2002) Redox-regulated molecular chaperones, *Cell. Mol. Life Sci. 59*, 1624−1631.
41. Huffman, D. L., and O'Halloran, T. V. (2001) Function, structure, and mechanism of intracellular copper trafficking proteins, *Annu. Rev. Biochem. 70*, 677−701.
42. Harford, C., and Sarkar, B. (1997) Amino terminal Cu(II)- and Ni(II)-binding (ATCUN) motif of proteins and peptides: Metal binding, DNA cleavage, and other properties, *Acc. Chem. Res. 30*, 123−130.
43. Zhang, Y., and Wilcox, D. E. (2002) Thermodynamic and spectroscopic study of Cu(II) and Ni(II) binding to bovine serum albumin, *J. Biol. Inorg. Chem. 7*, 327−337.
44. Leipe, D. D., Wolf, Y. I., Koonin, E. V., and Aravind, L. (2002) Classification and evolution of P-loop GTPases and related ATPases, *J. Mol. Biol. 317*, 41−72.
45. Zambelli, B., Stola, M., Musiani, F., De Vriendt, K., Samyn, B., Devreese, B., Van Beeumen, J., Turano, P., Dikiy, A., Bryant, D. A., and Ciurli, S. (2005) UreG, a chaperone in the urease assembly process, is an intrinsically unstructured GTPase that specifically binds Zn^{2+}, *J. Biol. Chem. 280*, 4684−4695.
46. Lu, J., Zheng, Y., Yamagishi, H., Odaka, M., Tsujimura, M., Maeda, M., and Endo, I. (2003) Motif CXCC in nitrile hydratase activator is critical for NHase biogenesis in vivo, *FEBS Lett. 553*, 391−396.
47. Benoit, S., and Maier, R. J. (2003) Dependence of *Helicobacter pylori* urease activity on the nickel-sequestering ability of the UreE accessory protein, *J. Bacteriol. 185*, 4787−4795.
48. Soriano, A., Colpas, G. J., and Hausinger, R. P. (2000) UreE stimulation of GTP-dependent urease activation in the UreD-UreF-UreG urease apoprotein complex, *Biochemistry 39*, 12435−12440.
49. Olson, J. W., Mehta, N. S., and Maier, R. J. (2001) Requirement of nickel metabolism proteins HypA and HypB for full activity of both hydrogenase and urease in *Helicobacter pylori*, *Mol. Microbiol. 39*, 176−182.

BI050993J